Catalysis Today xxx (2017) xxx–xxx

Contents lists available at ScienceDirect

Catalysis Today

journal homepage: www.elsevier.com/locate/cattod

Cascade engineered synthesis of 2-ethyl-1-hexanol from *n*-butanal and 2-methyl-1-pentanol from *n*-propanal using combustion synthesized Cu/Mg/Al mixed metal oxide trifunctional catalyst

Saurabh C. Patankar, Ganapati D. Yadav*

Department of Chemical Engineering, Institute of Chemical Technology, Nathalal Parekh Marg, Matunga, Mumbai, 400 019, India

ARTICLE INFO

Article history:
Received 20 July 2016
Received in revised form
22 November 2016
Accepted 3 January 2017
Available online xxx

Keywords:
Mixed metal oxide
Hydrotalcite
Copper
Trifunctional catalyst
2-Ethylhexanol
2-Methylpentanol
Cascade engineering

ABSTRACT

2-Ethyl-1-hexanol (2-EH) is a commercially important chemical that requires cost effective catalytic processes for synthesis. The cascade engineered synthesis of 2-EH was done in a single pot from *n*-butanal using solventless conditions with trifunctional mixed metal oxide containing 5% Cu and Mg/Al ratio of 3. This trifunctional catalyst was made by combustion synthesis technique which resulted in a porous network with narrow pore size distribution. The catalyst was characterized before and after reuse by FTIR, XRD, SEM, TEM, CO_2-TPD, NH_3-TPD, TPR, TGA and nitrogen BET analysis. The kinetics of reaction and selectivity profile of 2-EH are reported. The work was extended to one pot cascade engineered synthesis of 2-methyl-1-pentanol (2-MP) from *n*-propanal using the same catalyst. There was a significant effect of molecular size on rate of reaction and selectivity of the product. This is the first ever report on the one pot synthesis of 2-MP from *n*-propanal.

1. Introduction

Oxo alcohols are an important class of chemicals. 2-Ethyl-1-hexanol (2-EH) is traditionally used in production of plasticisers, coatings, adhesives and other speciality chemicals [1]. 2-Methyl-1-pentanol (2-MP) is used as solvent and also as an intermediate for production of valuable chemicals [2]. Oxo alcohols and 2-EH in particular find niche applications in the manufacture of acrylate and methacrylate esters, low volatility solvent for resins, waxes, animal fats, vegetable oils, disinfectants and as an additive in diesel fuels [3]. The consumption of 2-EH in India has grown by 55% in last five years with current net consumption of 0.12 million MT (Fig. ES1) [4]. The consumption is expected to grow further in next decade in developing countries of the world [5].

The traditional industrial production of 2-EH is a three step Dow LP process which involves aldol condensation of *n*-butanal using sodium hydroxide at 80–100 °C. This step is followed by dehydration and gas phase hydrogenation using Cu or Ni catalysts in a fixed bed reactor at 150 °C. Pure products are obtained by three stage distillation [6,7]. *n*-Butanal is made by the oxo-process from propylene. The production costs are high due to several reasons such as use of homogeneous catalysts involving multiple stages. Shell developed a one pot process with use of phosphate ligand modified cobalt/rhodium catalyst [8]. Apart from it, homogeneous co-catalyst like potassium hydroxide was also used [9–11]. Recently, the use of metal solid acid bifunctional catalysts was reported for direct synthesis of 2-ethyl-1-hexanol from *n*-butanal through aldol condensation-hydrogenation reactions integration. Co/Al_2O_3, Ru/Al_2O_3, Cu/Al_2O_3, Ni/Al_2O_3 and $Ni/Ce\text{-}Al_2O_3$ were used as catalyst [12]. We report one pot synthesis of 2-EH from *n*-butanal using a robust heterogeneous multifunctional catalyst, 5% Cu/MMO (mixed metal oxide containing 5% Cu and Mg/Al ratio of 3). The catalyst was made by combustion synthesis technique using glycerol as fuel. Combustion synthesis technique was found to be more robust than co-precipitation technique for synthesis of metal oxides by us and other research groups earlier [13–20]. The use of a heterogeneous catalyst and solvent less condition made the process cheaper and environmentally friendly than the traditional synthesis route. The cascade engineered synthesis of 2-EH using 5% Cu/MMO was studied. A reaction mechanism is proposed and kinetic model developed. The study was further extended to the synthesis of 2-MP from *n*-propanal to understand the effect of

* Corresponding author.
E-mail addresses: gdyadav@yahoo.com, gd.yadav@ictmumbai.edu.in (G.D. Yadav).

http://dx.doi.org/10.1016/j.cattod.2017.01.008
0920-5861/

Nomenclature

A	*n*-Butanal
B	2-Ethylhexenal
C	2-Ethylhexenol
D	Hydrogen
E	2-Ethyl-1-hexanol
F	Butanoic acid
G	Butyl butanoate
H	Butanol
I	*n*-Propanal
J	2-Methylpentenal
K	2-Methylpentenol
L	2-Methylpentanol
M	Propanoic acid
N	Propyl propanoate
O	Propanol
S_b	Base site
S_m	Metal site
S_a	Acid site
C_{Sm}	Concentration of metal site (mol cm^{-3})
C_{Sb}	Concentration of base site (mol cm^{-3})
C_{Sa}	Concentration of acid site (mol cm^{-3})
$K_{(A,I)m}$	Adsorption constant of *n*-butanal and *n*-propanal on metal site (cm^3 mol^{-1})
$K_{(A,I)b}$	Adsorption constant of *n*-butanal and *n*-propanal on base site (cm^3 mol^{-1})
$K_{(A,I)a}$	Adsorption constant of *n*-butanal and *n*-propanal on acid site (cm^3 mol^{-1})
$K_{(B,J)m}$	Adsorption constant of 2-ethylhexenal and 2-methylpentenal on metal site (cm^3 mol^{-1})
$K_{(B,J)b}$	Adsorption constant of 2-ethylhexenal and 2-methylpentenal on base site (cm^3 mol^{-1})
K_D	Adsorption constant of hydrogen on metal site (cm^3 mol^{-1})
$K_{(C,K)m}$	Adsorption constant of 2-ethylhexenol and 2-methylpentenol on metal site (cm^3 mol^{-1})
$K_{(E,L)m}$	Adsorption constant of 2-ethylhexanol and 2-methylpentanol on metal site (cm^3 mol^{-1})
$K_{(F,M)a}$	Adsorption constant of butanoic acid and propanoic acid on acid site (cm^3 mol^{-1})
$K_{(G,N)a}$	Adsorption constant of butyl butanoate and propyl propanoate on acid site (cm^3 mol^{-1})
$K_{(H,O)m}$	Adsorption constant of butanal and propanal on metal site (cm^3 mol^{-1})
K_X	Adsorption constant of water on acid site (cm^3 mol^{-1})
r_A	Rate of consumption of *n*-butanal (mol cm^{-3} min^{-1})
$k_{1,7}$	Rate constant of aldol condensation reaction (cm^3 mol^{-1} min^{-1})
$k_{2,8}$	Rate constant of hydrogenation reaction of alkenal to alkenol (cm^3 mol^{-1} min^{-1})
$k_{3,9}$	Rate constant of hydrogenation reaction of alkenol to aklanol (cm^3 mol^{-1} min^{-1})
$k_{4,10}$	Rate constant of acid hydrolysis reaction (cm^3 mol^{-1} min^{-1})
$k_{5,11}$	Rate constant of esterification reaction (cm^3 mol^{-1} min^{-1})
$k_{6,12}$	Rate constant of hydrogenation reaction of aldehyde (cm^3 mol^{-1} min^{-1})
k_{base}	Intrinsic constant pertaining to base sites (cm^6 mol^{-1} min^{-1} $g_{cat}{}^{-1}$)
k_{acid}	Intrinsic constant pertaining to acid sites (cm^6 mol^{-1} min^{-1} $g_{cat}{}^{-1}$)
k_{metal}	Intrinsic constant pertaining to metal sites (cm^6 mol^{-1} min^{-1} $g_{cat}{}^{-1}$)
W	Catalyst loading (g cm^{-3})

carbon chain length on the efficacy of the catalyst and to extend its utility in another industrially important reaction.

2. Experimental

2.1. Chemicals

Magnesium nitrate hexahydrate, aluminium nitrate nonahydrate, glycerol and copper(II) nitrate trihydrate were procured from S.D. Fine Chemicals Pvt. Ltd, Mumbai, India. *n*-Butanal and *n*-propanalwere procured from M/s. Thermo Fischer Scientific (India) Pvt. Ltd, Mumbai. Pure samples of 2-ethyl-1-hexanol and 2-methyl-1-pentanol were procured from Sigma Aldrich Chemicals Pvt. Ltd, Mumbai.

2.2. Catalyst synthesis

Saturated aqueous solution of magnesium nitrate hexahydrate (0.024 mol) and aluminium nitrate nonahydrate (0.008 mol) was made such that the molar ratio of Mg:Al was 3. Copper (II) nitrate trihydrate (1.17 mmol) was then added to the mixture such that the loading of copper on hydrotalcite was 5% (w/w). Glycerol (0.025 mol) was used as a fuel and mixed with the nitrate solution [13]. The slurry was heated at 80 °C for 30 min. The thick slurry was later kept in preheated muffle furnace at 500 °C and allowed to combust. The voluminous material formed post combustion was used as a catalyst and designated as Cu/MMO.

2.3. Catalyst characterization

The synthesized catalyst was characterized per se and after use to understand the structure activity relationship. Temperature programmed desorption (TPD) was used with CO_2 and NH_3 as probe molecules to understand the nature of basic and acidic sites on the catalyst (AutoChem II 2910, Micromeretics, USA). Twenty mg catalyst sample was heated to 500 °C in quartz tube under flow of helium to remove traces of moisture, air and any other organic compounds in case of used catalyst [21–23]. 10% (w/w) Ammonia in helium was then adsorbed on the catalyst surface. The physisorbed gas was desorbed with flow of helium. The chemisorbed gas was desorbed using a temperature program and measured using a thermal conductivity detector (TCD). The same procedure was repeated for CO_2-TPD experiments with use of 10% (w/w) carbon dioxide in helium. Temperature programmed reduction (TPR) was studied to understand the strength of metal sites. Catalyst sample (20 mg) was heated to 500 °C under 5% O_2 in helium so that the catalyst was completely oxidised [24]. The traces of O_2 were removed by flow of helium and the catalyst sample cooled to room temperature. 10% (w/w) hydrogen in argon was then passed over the catalyst by heating the catalyst to 500 °C. The hydrogen uptake was measured using a TCD. FTIR spectra was obtained from the catalyst sample pressed in KBr pellet to understand the bending and stretching vibrations (Perkin Elmer, 1000-PC). The analysis was done in the fingerprint region from wavenumber of 400–4000 cm^{-1} at a resolution of 2 cm^{-1}. Powder X-ray Diffraction (XRD) was used to understand the crystallinity of the catalyst (Bruker D8 Advance, USA). Analysis was done using Cu kα radiations with beam current of 40 kV and

Please cite this article in press as: S.C. Patankar, G.D. Yadav, Cascade engineered synthesis of 2-ethyl-1-hexanol from *n*-butanal and 2-methyl-1-pentanol from *n*-propanal using combustion synthesized Cu/Mg/Al mixed metal oxide trifunctional catalyst, Catal. Today (2017), http://dx.doi.org/10.1016/j.cattod.2017.01.008

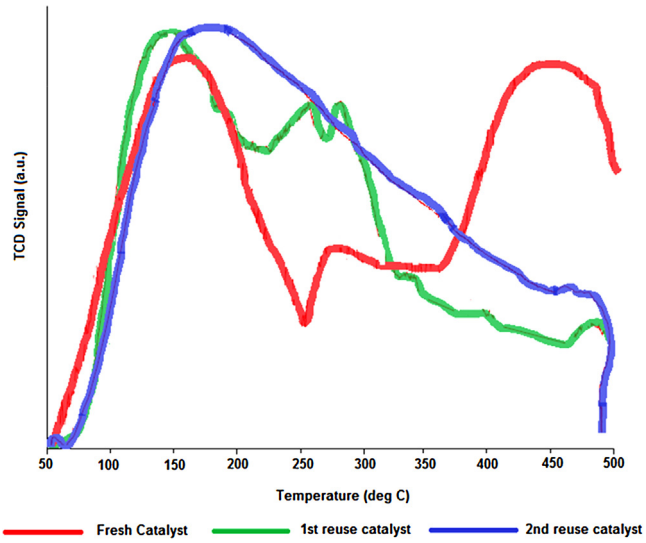

Fig. 1. CO_2-TPD study on fresh and used 5% Cu/MMO catalyst.

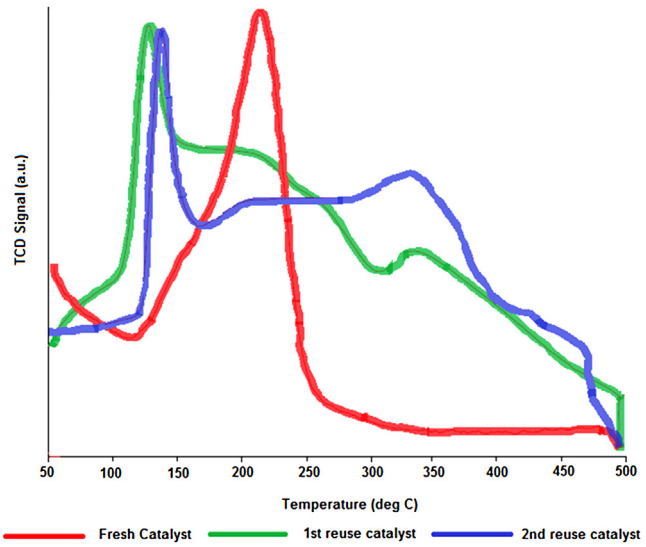

Fig. 3. TPR studies on fresh and used 5% Cu/MMO catalyst.

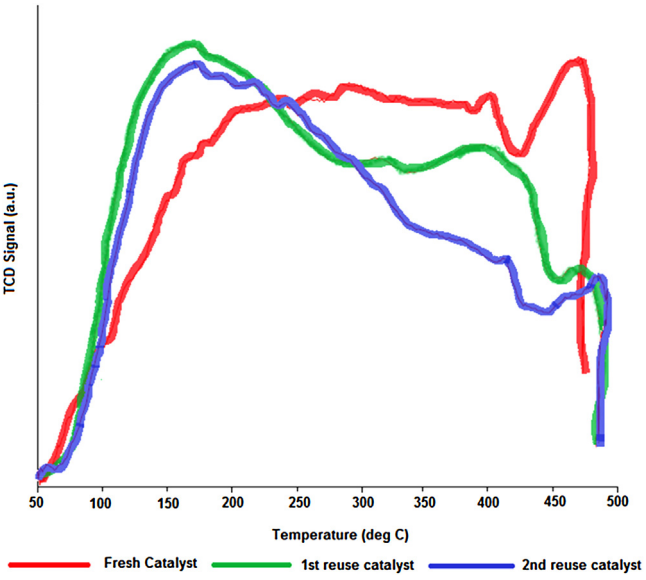

Fig. 2. NH_3-TPD studies on fresh and used 5% Cu/MMO catalyst.

100 mA from 2θ value of 2°–80°. The surface properties of the catalyst were studied using nitrogen BET and BJH methods for surface area and pore size distribution (ASAP 2020, Micromeritics, USA). Catalyst sample (200 mg) was degassed at 350 °C under vacuum for 4 h. Scanning electron microscopy (SEM) was used to study the surface morphology of the catalyst (JEOL, JSM-7500F, Japan). The catalyst sample was mounted on specimen stud and coated with platinum to prevent charring during imaging. Transmission electron microscopy (TEM) was used to analyse the location of catalyst components. The catalyst sample was dispersed in ethanol solution and a few drops of suspension were put on 400-mesh, 3.5 mm Cu grid. Theromogravimetric analysis (TGA) was used to study the stability of catalyst up to 600 °C (TA Instruments, TGA Q500 with auto sampler).

2.4. Catalytic testing

The experiments for 2-EH and 2-MP synthesis were done in a 100 ml batch reactor (Amar equipments, Mumbai). The reactor had a 45° pitched bladed turbine impeller, a temperature controller (±1° C), a pressure gauge and a speed regulator. In a typical experiment for 2-EH synthesis, 0.4 mol *n*-butanal was charged into the reactor along with *n*-decane (100 μl) as internal standard and required quantity of Cu/MMO catalyst. The reactor was purged with nitrogen to remove traces of air and then pressurized with hydrogen at a particular pressure which was maintained throughout the experiment. The reactor was then heated to the desired temperature [25]. Samples were withdrawn periodically and analysed by GC (Chemito C1000) equipped with BPX-50 capillary column (0.25 μm × 0.25 mm × 30 m with 50% diphenyl-50% dimethylpolysiloxane packing) and FID. The synthesis of 2-EH was confirmed by matching the residence time of pure sample. For the synthesis of 2-MP, 0.4 mol of *n*-propanal was used as the reactant using the same experimental procedure and technique for confirmation of product as used for synthesis of 2-EH.

3. Results and discussion

3.1. Catalyst characterization

Combustion synthesis technique gave the Cu/MMO catalyst a distinct morphology. The transition metal nitrates and alkali metal nitrates decomposed at different temperatures to form the Cu/MMO catalyst. When the aqueous solution containing nitrate precursors and fuel was placed in the preheated muffle furnace, the decomposition of different components occurred sequentially. The decomposition temperatures of transition metal nitrates are less than alkali metal nitrates due to back donation of electron cloud from nitrate to unfilled d-orbital of transition metals [26,27]. The decomposition occurred in the following sequence: copper (II) nitrate trihydrate (170° C), aluminium nitrate nonahydrate (250° C) and magnesium nitrate hexahydrate (330° C). Due to this sequence, copper was loaded inside the porous mixed metal oxide. There are previous studies which report XPS analysis of hydrotalcite derived metal oxides containing copper. An in situ XPS/XAES study done on Cu/Mg/Al mixed oxide derived from hydrotalcite reported that copper in its reduced form exists as small clusters inside hydrotalcite matrix [28]. This observation is also supported by an EXAFS (extended X-ray absorption fine structure) study [29]. It has also been reported that surface concentration of copper decreases after calcination and reduction in copper substituted hydrotalcite. It is attributed to complex process of surface reconstruction during calcination and reduction [30,31]. The TEM image of calcined and

Please cite this article in press as: S.C. Patankar, G.D. Yadav, Cascade engineered synthesis of 2-ethyl-1-hexanol from *n*-butanal and 2-methyl-1-pentanol from *n*-propanal using combustion synthesized Cu/Mg/Al mixed metal oxide trifunctional catalyst, Catal. Today (2017), http://dx.doi.org/10.1016/j.cattod.2017.01.008

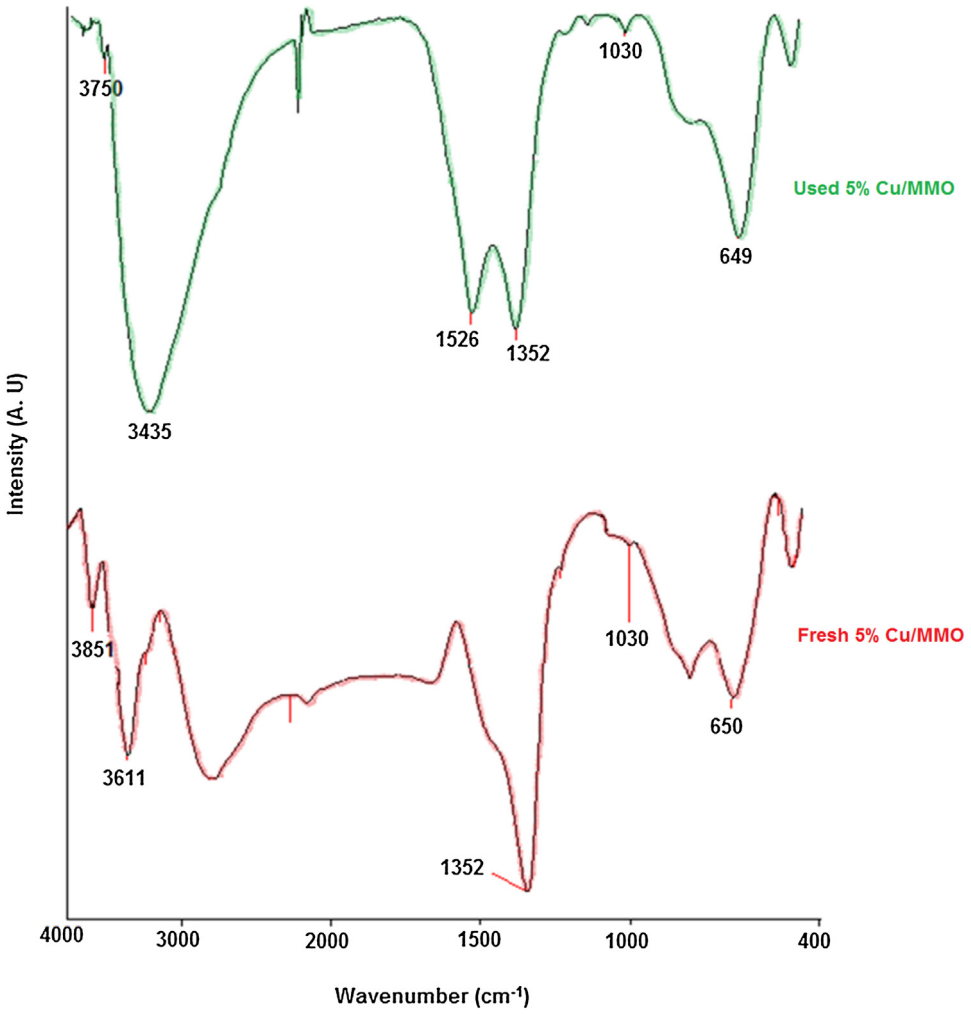

Fig. 4. FTIR spectra of fresh and used 5% Cu/MMO catalyst.

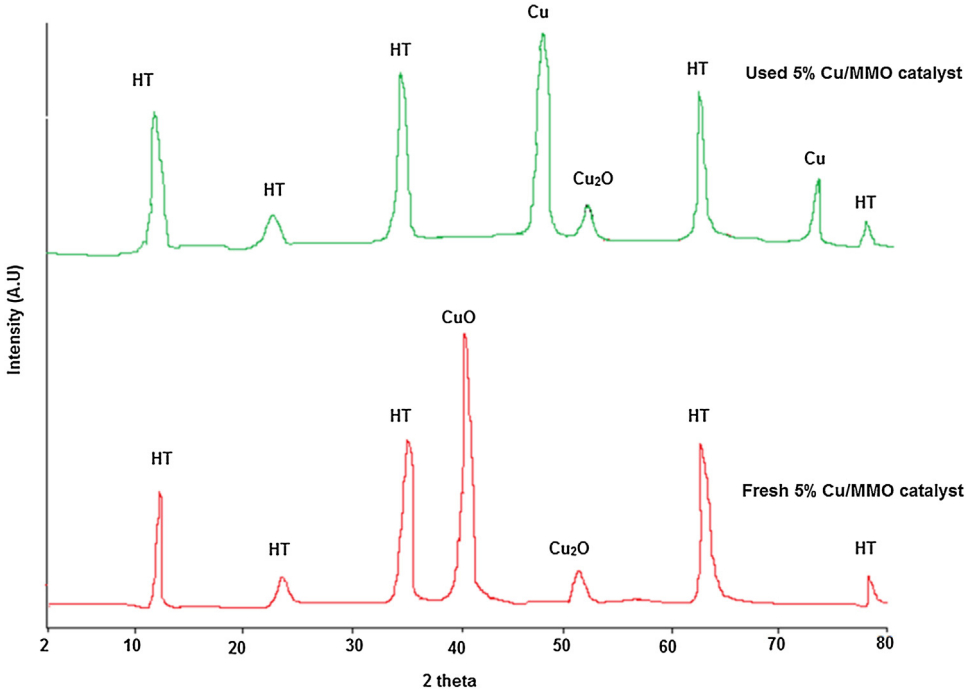

Fig. 5. XRD pattern of fresh and used 5% Cu/MMO catalyst.

Please cite this article in press as: S.C. Patankar, G.D. Yadav, Cascade engineered synthesis of 2-ethyl-1-hexanol from *n*-butanal and 2-methyl-1-pentanol from *n*-propanal using combustion synthesized Cu/Mg/Al mixed metal oxide trifunctional catalyst, Catal. Today (2017), http://dx.doi.org/10.1016/j.cattod.2017.01.008

Table 1
Temperature programmed desorption and temperature programmed reduction analysis of 5% Cu/MMO catalyst.

a) CO_2-TPD analysis of fresh and used 5% Cu/MMO catalyst

Usage of 5% Cu/MMO catalyst	Strength of basic sites (mmol/g_{cat})
Fresh	1.07
1st reuse	0.47
2nd reuse	0.47

b) NH_3-TPD analysis of fresh and reused 5% Cu/MMO catalyst

Usage of 5% Cu/MMO catalyst	Strength of acidic sites (mmol/g_{cat})
Fresh	0.55
1st reuse	0.50
2nd reuse	0.48

c) TPR analysis of fresh and used 5% Cu/MMO catalyst

Usage of 5% Cu/MMOcatalyst	Strength of metal sites (mmol/g_{cat})
Fresh	8.68
1st reuse	7.83
2nd reuse	7.34

reduced 5% Cu/MMO catalyst reveals Cu nanoparticles reside inside mixed metal oxide matrix (Fig. ES2).

The 5% Cu/MMO catalyst had base, acid and metal functionalities as observed from CO_2-TPD, NH_3-TPD and TPR results. In the case of fresh catalyst, CO_2 was desorbed in the temperature range of 150 °C and 450 °C indicating presence of strong base sites. The elution occurred up to 300 °C in case of used catalyst indicating change in the concentration of base site. However, the basicity remained the same on further reuse (Fig. 1). The values of CO_2-TPD for fresh and used catalysts are listed in Table 1a. For NH_3- TPD, desorption of NH_3 occurred in temperature range of 200–400 °C both in fresh and used catalyst (Fig. 2). The values of NH_3-TPD for fresh and used catalysts are listed in Table 1b. There was no change in acid site concentration as acid sites were not involved in the selective synthesis route to yield 2-EH from *n*-butanal. The TPR results indicated that H_2 uptake occurred at 200 °C in fresh catalyst while it occurred from 150 °C in used catalyst with small uptake at 350 °C (Fig. 3). The amount of hydrogen uptake in fresh and used catalyst is listed in Table 1c. The FTIR spectra of fresh and used catalyst showed Cu-O bending at 650 cm^{-1} (Fig. 4). The N—O stretch was seen at 1352 cm^{-1} in fresh catalyst and at 1352 cm^{-1} and 1526 cm^{-1} in the case of used catalyst. The two bands for N—O stretch were seen in used catalyst due to deformation of interlayer space. The hydrogen bonded hydroxyl groups are seen in both cases beyond 3300 cm^{-1} [32]. XRD patterns of fresh catalyst showed that the catalyst was reduced in-situ during reaction. The Cu_2O phase did not participate in the reaction and was retained. It is seen in fresh and used catalyst at 25°. The peak at 2θ value of 12° is attributed to MgO-Al_2O_3 phase. CuO is represented by peak at 35° in fresh catalyst sample only. The Cu peaks are seen in the diffraction pattern of used catalyst at 39° and 71° (Fig. 5). In the case of fresh catalyst, a sharp pore size distribution was observed at 35 A° (Fig. 6). The fresh catalyst showed uniform pores spread over the entire surface of the catalyst. The uniform pore size distribution in 5% Cu/MMO catalyst is attributed to the solution combustion synthesis technique used for the synthesis of catalyst [33,34]. Uniform pore size distribution has been reported for materials like Mg-Al hydrotalcite, Cu/Cr hydrotalcite like compounds, calcined hydrotalcite supported on hexagonal silica, and Co-Mn-Mg-Al mixed oxide spinel catalysts [35–39]. The small pores were blocked after the reaction. Hence the average pore size increased after reaction. The observation of change in pore size distribution was supported from SEM images (Figs. Fig. 7and ES3). However, the surface area and pore volume did not change significantly (Table 2). As the small pores were blocked after the

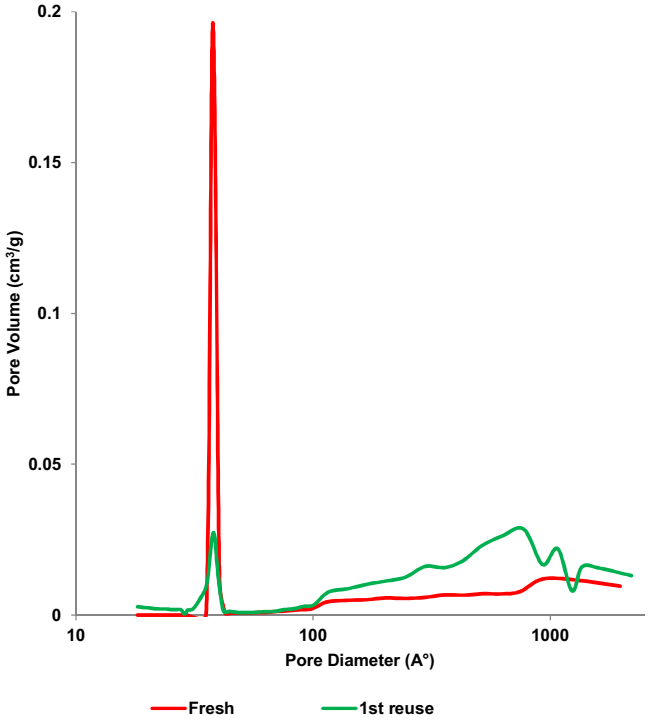

Fig. 6. Pore size distribution in fresh and used 5% Cu/MMO catalyst.

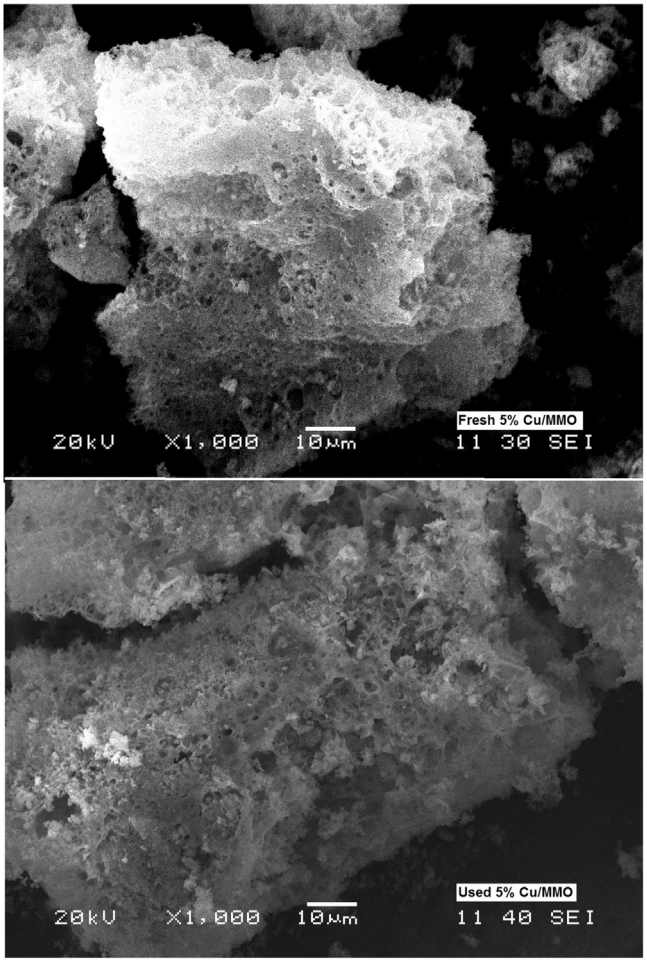

Fig. 7. SEM images of fresh and used 5% Cu/MMO catalyst.

Please cite this article in press as: S.C. Patankar, G.D. Yadav, Cascade engineered synthesis of 2-ethyl-1-hexanol from *n*-butanal and 2-methyl-1-pentanol from *n*-propanal using combustion synthesized Cu/Mg/Al mixed metal oxide trifunctional catalyst, Catal. Today (2017), http://dx.doi.org/10.1016/j.cattod.2017.01.008

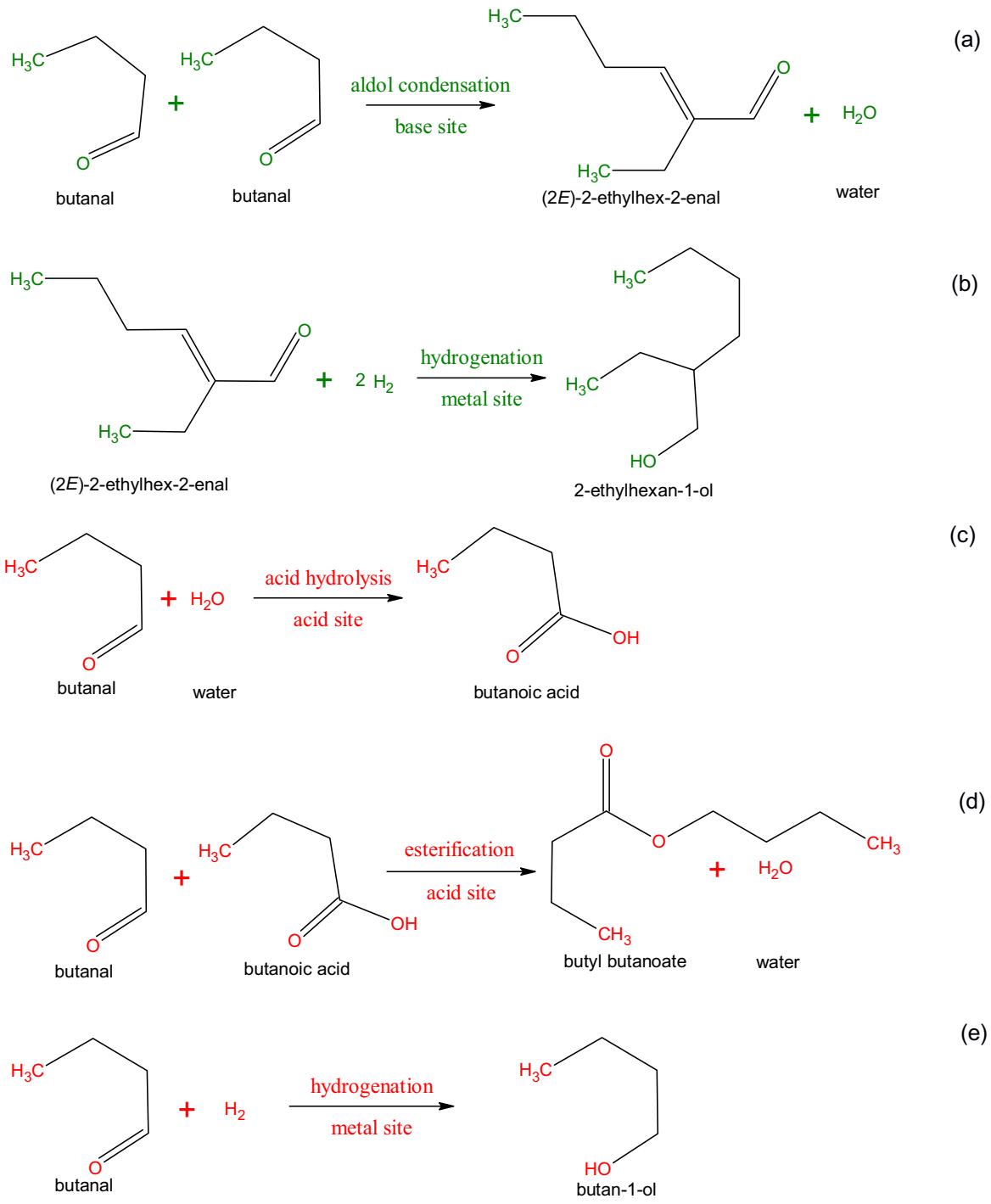

Scheme 1. Consecutive and parallel reactions during one pot synthesis of 2-EH.

Table 2
Porosimetry analysis of 5% Cu/MMO catalyst.

5% Cu/MMO catalyst	Surface area (m^2/g)	Pore size (nm)	Pore volume (cm^3/g)
Fresh	190	5.3	0.32
1st reuse	188	10.7	0.37
2nd reuse	188	11.2	0.37

reaction, the catalytic sites in the small pores were inaccessible. This is evident from change in the values of CO_2- TPD, NH_3-TPD and TPR analysis of fresh and used catalyst. The TGA profile (Fig. ES4) indicates that catalyst is stable up to 600 °C. The initial weight loss was due to moisture adsorbed in pores and on the surface of catalyst.

3.2. Theoretical aspects of 2-EH synthesis

The possible reactions during the one pot synthesis of 2-EH from *n*-butanal are listed in the Scheme 1 and are follows: Aldol condensation of *n*-butanal on base sites to form 2-ethylhexenal (reaction a), hydrogenation of 2-ethylhexenal to form 2-EH (reaction b), acid hydrolysis of *n*-butanal with the water released during aldol condensation to form butanoic acid (reaction c), esterification of *n*-butanal and butanoic acid on acid site to form butyl butanoate

Please cite this article in press as: S.C. Patankar, G.D. Yadav, Cascade engineered synthesis of 2-ethyl-1-hexanol from *n*-butanal and 2-methyl-1-pentanol from *n*-propanal using combustion synthesized Cu/Mg/Al mixed metal oxide trifunctional catalyst, Catal. Today (2017), http://dx.doi.org/10.1016/j.cattod.2017.01.008

(reaction d), hydrogenation of *n*-butanal to form 1-butanol (reaction e). The reactions (a) and (b) are desired while (c)–(e) are undesired. Reactions (a) and (b) are consecutive reactions while (c)–(e) are parallel steps. To ascertain the active sites on 5% Cu/MMO catalyst and their role, aldol condensation of *n*-butanal was performed on mixed oxide catalyst with only MgO and Al_2O_3 in molar ratio of Mg:Al = 3 in presence of hydrogen. The product at the end of reaction was 2-ethylhexenal only, which is aldol condensation product from *n*-butanal. The same reaction was performed using 5% Cu/MMO catalyst in presence of nitrogen. The end product was observed to be 2-ethylhexenal. This observation ascertained that MgO-Al_2O_3 phase was responsible for base catalysed aldol condensation reaction and Cu sites did not contribute in aldol condensation reaction. *n*-Butanal in otherwise same conditions was allowed to react in presence of hydrogen on 5% Cu/C catalyst. The end product was observed to be 1-butanol only. Thus it was evident that Cu was responsible for metal sites leading to hydrogenation reaction. To ascertain the role of acidic sites, *n*-butanal in otherwise same conditions was allowed to react in presence of hydrogen on 5% Cu/MgO catalyst. In this case, the undesired reactions of acid hydrolysis and esterification did not occur as MgO has only basic sites thus yielding better selectivity of 80% towards 2-ethyl-1-hexanol after 1 h of reaction. Several studies earlier have reported use of Cu as hydrogenation catalyst. Aqueous phase catalytic hydrogenation of furfural to cyclopentanol have been reported over Cu-Mg-Al hydrotalcite derived catalysts [40]. Cu supported on hydrotalcite has been used as catalyst for hydrogenation of levulinic acid and furfural [41]. Cu-Mg-Al mixed oxide has been used for hydrogenation of cinnamaldehyde [42]. Liquid phase transfer hydrogenation of furfural to furfuryl alcohol has been reported on Cu-Mg-Al catalyst [43]. 5% Cu/MMO catalyst was so tailored that the base site activity was the highest followed by activity of metal sites and acid sites. Therefore, the aldol condensation of *n*-butanal on base sites occurred first rather than hydrogenation of *n*-butanal. 2-EH was formed selectively after the start of the reaction up to 30 min. As the aldehyde was consumed, there was no competitive adsorption of aldehyde on base sites of the catalyst. As the rate of aldol condensation decreased, the rate of acid hydrolysis on acid sites and hydrogenation of aldehyde on metal sites became significant and selectivity towards 2-EH decreased with time. Hence it was essential to calculate instantaneous selectivity of 2-EH and develop mathematical expression for change in selectivity. For developing the equation for instantaneous selectivity, following steps were assumed.

1. Adsorption of *n*-butanal on base site

$$A + S_b \overset{K_{Ab}}{\leftrightarrow} A.S_b \quad (1)$$

2. Aldol condensation of adsorbed *n*-butanal (A) on adjacent base sites to form 2-ethylhexenal (B) and water (X)

$$A.S_b + A.S_b \overset{k_1}{\rightarrow} B.S_b + X.S_b \quad (2)$$

3. Dissociative adsorption of hydrogen (D) on metal site

$$D + 2S_m \overset{K_D}{\leftrightarrow} 2\sqrt{D}.S_m \quad (3)$$

4. Migration of 2-ethylhexenal (B) from base site to metal site

$$B.S_b \overset{K_B}{\leftrightarrow} B.S_m \quad (4)$$

5. Hydrogenation of adsorbed 2-ethylhexenal (B) on metal site to form 2-ethylhexenol (C)

$$B.S_m + \sqrt{D}.S_m \overset{k_2}{\rightarrow} C.S_m + S_m \quad (5)$$

6. Hydrogenation of 2-ethylhexenol (C) on metal site to form 2-ethylhexanol (E)

$$C.S_m + \sqrt{D}.S_m \overset{k_3}{\rightarrow} E.S_m + S_m \quad (6)$$

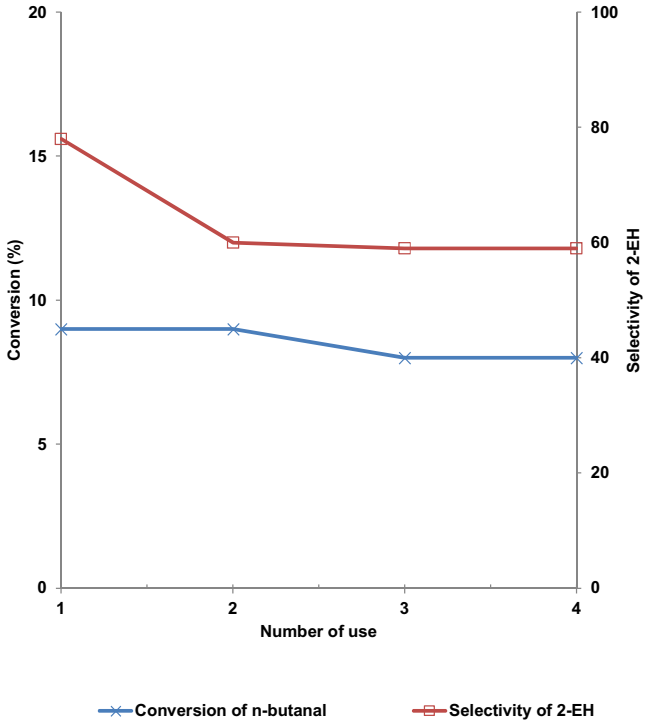

Fig. 8. Reusability of 5% Cu/MMO catalyst for 2-EH synthesis *n*-butanal 0.4 mol, Speed of agitation: 1000 rpm, Temperature: 150 °C, Catalyst loading: 0.05 g/cm^3, reaction time 30 min.

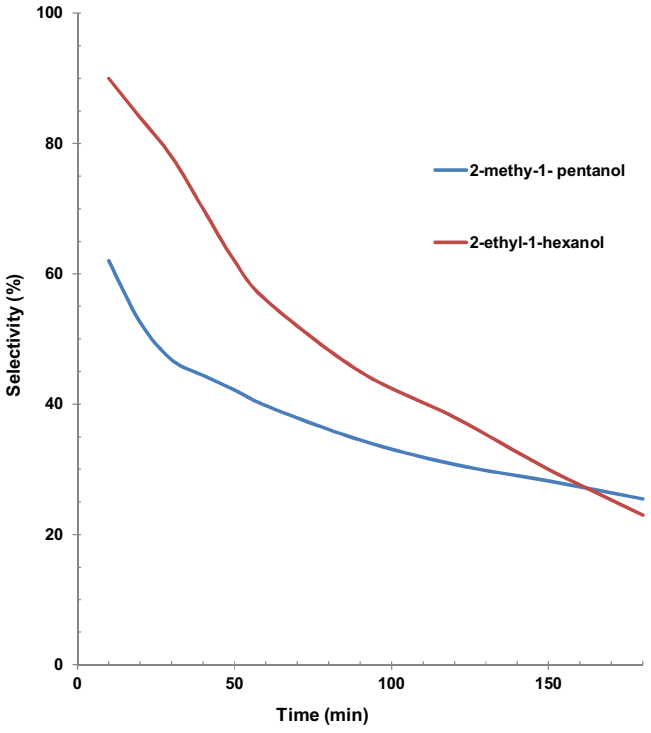

Fig. 9. Difference in selectivity of 2-EH and 2-MP using 5% Cu/MMO catalyst for synthesis from *n*-butanal and *n*-propanal respectively.

7. Desorption of 2-EH (E) from metal site

$$E.S_m \overset{1/K_E}{\leftrightarrow} E + S_m \quad (7)$$

8. Adsorption of *n*-butanal (A) on acid site

$$A + S_a \overset{K_{Aa}}{\leftrightarrow} A.S_a \quad (8)$$

Please cite this article in press as: S.C. Patankar, G.D. Yadav, Cascade engineered synthesis of 2-ethyl-1-hexanol from *n*-butanal and 2-methyl-1-pentanol from *n*-propanal using combustion synthesized Cu/Mg/Al mixed metal oxide trifunctional catalyst, Catal. Today (2017), http://dx.doi.org/10.1016/j.cattod.2017.01.008

9. Adsorption of water (X) on acid site

$$X + S_a \overset{K_X}{\leftrightarrow} X.S_a \tag{9}$$

10. Acid hydrolysis of adsorbed*n*-butanal (A) and water (X) on acid site to form butanoic acid (F)

$$A.S_a + X.S_a \overset{k_3}{\rightarrow} F.S_a + S_a \tag{10}$$

11. Esterification of adsorbed *n*-butanal (A) and butanoic acid (F) to form butyl butanoate (G)

$$A.S_a + F.S_a \overset{k_4}{\rightarrow} G.S_a + S_a \tag{11}$$

12. Desorption of butyl butanoate (G) from acid site

$$G.S_a \overset{1/K_G}{\leftrightarrow} G + S_a \tag{12}$$

13. Adsorption of *n*-butanal (A) on metal site

$$A + S_m \overset{K_{Am}}{\leftrightarrow} A.S_m \tag{13}$$

14. Hydrogenation of adsorbed *n*-butanal and hydrogen to form butanol (H)

$$A.S_m + \sqrt{D}.S_m \overset{k_6}{\rightarrow} H.S_m + S_m \tag{14}$$

15. Desorption of butanol (H) from metal site

$$H.S_m \overset{1/K_H}{\leftrightarrow} H + S_m \tag{15}$$

The instantaneous selectivity was dependent on the relative rate of aldol condensation reaction (reaction a) and rates of acid hydrolysis reaction (reaction c), esterification reaction (reaction d) and direct hydrogenation of *n*-butanal (reaction e).

$$S_{\left(\frac{a}{c+d+e}\right)} = \frac{k_1 C_{A.Sb}^2}{\left(k_4 C_{A.Sa} C_{X.Sa} + k_5 C_{A.Sa} C_{F.Sa} + k_6 C_{A.Sm} C_{\sqrt{D}.Sm}\right)} \tag{16}$$

$$S_{\left(\frac{a}{c+d+e}\right)} = \frac{k_1 K_{Ab}^2 C_A^2 C_{Sb}^2}{\left(k_4 K_{Aa} K_X C_A C_X C_{Sa}^2 + k_5 K_{Aa} K_F C_A C_F C_{Sa}^2 + k_6 K_{Am} C_A \sqrt{K_D C_D} C_{Sm}^2\right)} \tag{17}$$

Site balance for base site, acid site and metal site is as follows:

$$C_{tb} = \left(1 + K_{Ab} C_A + K_{Bb} C_B\right) C_{Sb} \tag{18}$$

$$C_{ta} = \left(1 + K_{Aa} C_A + K_X C_X + K_F C_F + K_G C_G\right) C_{Sa} \tag{19}$$

$$C_{tm} = \left(1 + K_{Am} C_A + K_{Bm} C_B + K_C C_C + \sqrt{K_D C_D} + K_E C_E + K_H C_H\right) C_{Sm} \tag{20}$$

Substituting Eq. (17)–(19) in Eq. (16),

$$S_{\left(\frac{a}{c+d+e}\right)} = \frac{\frac{k_1 K_{Ab}^2 C_A^2 C_{tb}^2}{\left(1+K_{Ab}C_A+K_{Bb}C_B\right)^2}}{\left(\frac{k_4 K_{Aa} K_X C_A C_X + k_5 K_{Aa} K_F C_A C_F}{\left(1+K_{Aa}C_A+K_X C_X+K_F C_F+K_G C_G\right)^2} C_{ta}^2 + \frac{k_6 K_{Am} C_A \sqrt{K_D C_D} C_{tm}^2}{\left(1+K_{Am}C_A+K_{Bm}C_B+K_C C_C+\sqrt{K_D C_D}+K_E C_E+K_H C_H\right)^2}\right)} \tag{20}$$

The values of rate constants and adsorption constants for all reactions were determined from experimental data by interpolation (Tables ES1 and ES3). The parity plot of theoretical and experimental values of selectivity of 2-EH showed agreement (Fig. ES5). The random nature of the residual plot indicated validation of the derived expression (Fig. ES6).

For calculating the rate of consumption of *n*-butanal, all four parallel reactions wherein *n*-butanal was consumed were considered. The rate expression for the initial rate of reaction was,

$$-r_{Ai} = k_1 C_{A.Sb}^2 + k_4 C_{A.Sa} C_{X.Sa} + k_5 C_{A.Sa} C_{F.Sa} + k_6 C_{A.Sm} C_{\sqrt{D}.Sm} \tag{21}$$

$$-r_{Ai} = k_1 K_{Ab}^2 C_A^2 C_{Sb}^2 + k_4 K_{Aa} K_X C_A C_X C_{Sa}^2 + k_5 K_{Aa} K_F C_A C_F C_{Sa}^2 + k_6 K_{Am} C_A \sqrt{K_D C_D} C_{Sm}^2 \tag{22}$$

Substituting Eq. (17)–(19) in Eq. (22),

$$-r_{Ai} = \frac{k_1 K_{Ab}^2 C_A^2 C_{tb}^2}{\left(1 + K_{Ab} C_A + K_{Bb} C_B\right)^2} + \frac{\left(k_4 K_{Aa} K_X C_A C_X + k_5 K_{Aa} K_F C_A C_F\right) C_{ta}^2}{\left(1 + K_{Aa} C_A + K_X C_X + K_F C_F + K_G C_G\right)^2} + \frac{k_6 K_{Am} C_A \sqrt{K_D C_D} C_{tm}^2}{\left(1 + K_{Am} C_A + K_{Bm} C_B + K_C C_C + \sqrt{K_D C_D} + K_E C_E + K_H C_H\right)^2} \tag{23}$$

$$-r_{Ai} = \frac{k_1 K_{Ab}^2 C_A^2 K_{base} W}{\left(1 + K_{Ab} C_A + K_{Bb} C_B\right)^2} + \frac{\left(k_4 K_{Aa} K_X C_A C_X + k_5 K_{Aa} K_F C_A C_F\right) K_{acid} W}{\left(1 + K_{Aa} C_A + K_X C_X + K_F C_F + K_G C_G\right)^2} + \frac{k_6 K_{Am} C_A \sqrt{K_D C_D} K_{metal} W}{\left(1 + K_{Am} C_A + K_{Bm} C_B + K_C C_C + \sqrt{K_D C_D} + K_E C_E + K_H C_H\right)^2} \tag{24}$$

$$C_{tb}^2 = K_{base} W, \quad C_{ta}^2 = K_{acid} W \quad \text{and} \quad C_{tm}^2 = K_{metal} W$$

Where W was catalyst loading in g/cm^3.

The rate constants of hydrogenation reaction were calculated as follows:

$$\frac{dC_C}{dt} = k_2 C_{B.Sm} C_{\sqrt{D}.Sm} + k_3 C_{E.Sm} C_{Sm} \tag{25}$$

At equilibrium after 3 h of reaction,

$$k_2 C_{B.Sm} C_{\sqrt{D}.Sm} + k_3 C_{E.Sm} C_{Sm} = 0$$

$$k_2 K_{Bm} \sqrt{K_D C_D} C_B C_{Sm}^2 + k_3 K_E C_E C_{Sm}^2 = 0$$

$$k_2 K_{Bm} \sqrt{K_D C_D} C_B + k_3 K_E C_E = 0 \tag{28}$$

The values of intrinsic constants were also determined by interpolation using the experimental data at different temperatures and catalyst loading (Table ES3). The mechanism to selectively synthesize 2-EH is shown pictorially in Scheme 2.

3.3. Experimental aspects of 2-EH synthesis

Experiments were done by varying hydrogen pressure from 5 to 50 kg/cm^2 to understand its effect on rate of reaction and selectivity of 2-EH. There was no significant effect on either the rate of reaction or the selectivity of 2-EH. The hydrogenation reaction is faster than the aldol condensation reaction as seen from the rate constant values as well (Table ES1). Experiments were then carried out by changing the speed of agitation from 800 to 1200 rpm. There was no change in the initial rate of reaction beyond 1000 rpm. Thus, there was no mass transfer limitation beyond 1000 rpm. The Wiesz-Prater modulus were calculated over the entire time of reaction considering the average particle size of catalyst as 100 μm and pore size 10 nm. The tortuosity was assumed to be 3 and diffusivity was calculated to be 10×10^{-8} cm^2/min. Over the entire time of reaction, the Wiesz-Prater moduli were below unity and hence the reaction was intrinsically kinetically controlled. The effect of catalyst loading was studied on the initial rate of reaction by varying the catalyst loading from 0.025 to 0.075 g/cm^3. The rate of reaction increased with the increase in catalyst loading (Fig. ES7). This indicated the dependence of the reaction on the number of active sites. The temperature was varied from 110° to 170° C. The initial rate of

Please cite this article in press as: S.C. Patankar, G.D. Yadav, Cascade engineered synthesis of 2-ethyl-1-hexanol from *n*-butanal and 2-methyl-1-pentanol from *n*-propanal using combustion synthesized Cu/Mg/Al mixed metal oxide trifunctional catalyst, Catal. Today (2017), http://dx.doi.org/10.1016/j.cattod.2017.01.008

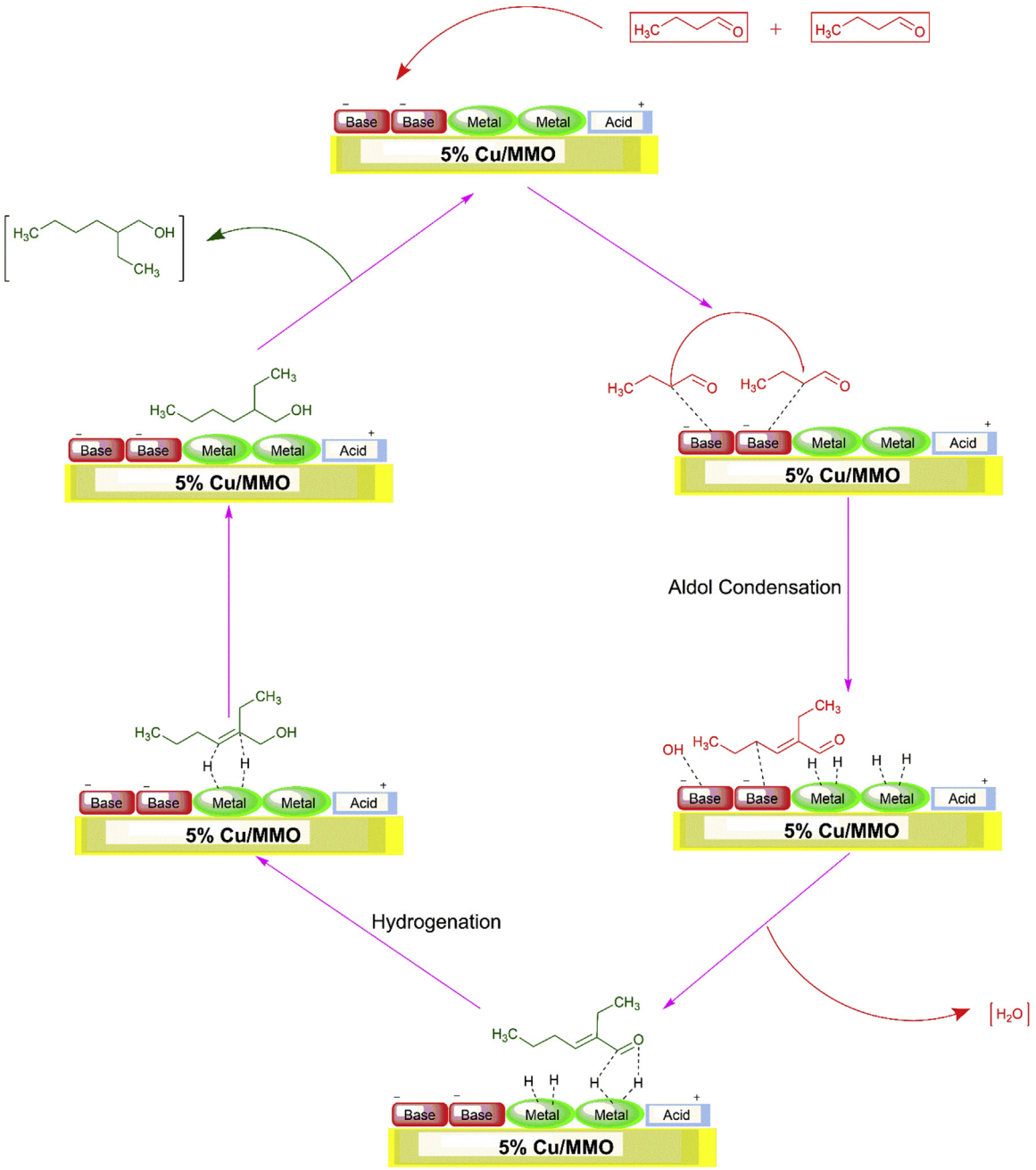

Scheme 2. Mechanism for selective synthesis of 2-EH from *n*-butanal using 5 % Cu/MMO catalyst.

reaction increased with the increase in temperature (Fig. ES8). The values of rate constants obtained at different temperatures were used to calculate the activation energy for the aldol condensation reaction. The activation energy was found to be 9.2 kcal/mol (Table ES1). The reusability of the catalyst was studied by reusing the catalyst for 3 cycles. After each experiment, the catalyst was filtered out from the reactor and washed with methanol under reflux conditions at 90 °C. It was dried and then used in next reaction as it is. The rate of reaction for selective synthesis of 2-EH from *n*-butanal was low. Conversion of *n*-butanal after 3 h was 30%. The selectivity of 2-EH decreased with time and was 23% at end of 3 h. Hence recycle studies were carried out after performing reaction for 30 min in batch reactor when selectivity of 2-EH was significant at 75%. The best way to operate the process for higher yield of 2-EH is to use a packed bed reactor and recycle the reaction mixture. The catalyst pore structure undergoes a transformation as elaborated in characterization results after the first use. However, the performance of catalyst remained stable in further uses. (Fig. 8).

3.4. *Synthesis of 2-MP from* n-*propanal*

The synthesis of 2-MP was studied by performing separate experiments with *n*-propanal as the starting material and Cu/MMO catalyst. All the experiments were repeated with unless otherwise the same conditions used for 2-EH synthesis. The objective was to study the effect of carbon chain length on the efficacy of the catalyst. The series and parallel reactions occurring during one pot 2-MP synthesis were similar to the reactions which occurred for 2-EH synthesis (Scheme 3) viz, aldol condensation of *n*-propanal to form 2-methylpentenal (reaction f), hydrogenation of 2-methylpentenal to form 2-MP (reaction g), acid hydrolysis of *n*-propanal to form propanoic acid (reaction h), esterification of *n*-

Please cite this article in press as: S.C. Patankar, G.D. Yadav, Cascade engineered synthesis of 2-ethyl-1-hexanol from *n*-butanal and 2-methyl-1-pentanol from *n*-propanal using combustion synthesized Cu/Mg/Al mixed metal oxide trifunctional catalyst, Catal. Today (2017), http://dx.doi.org/10.1016/j.cattod.2017.01.008

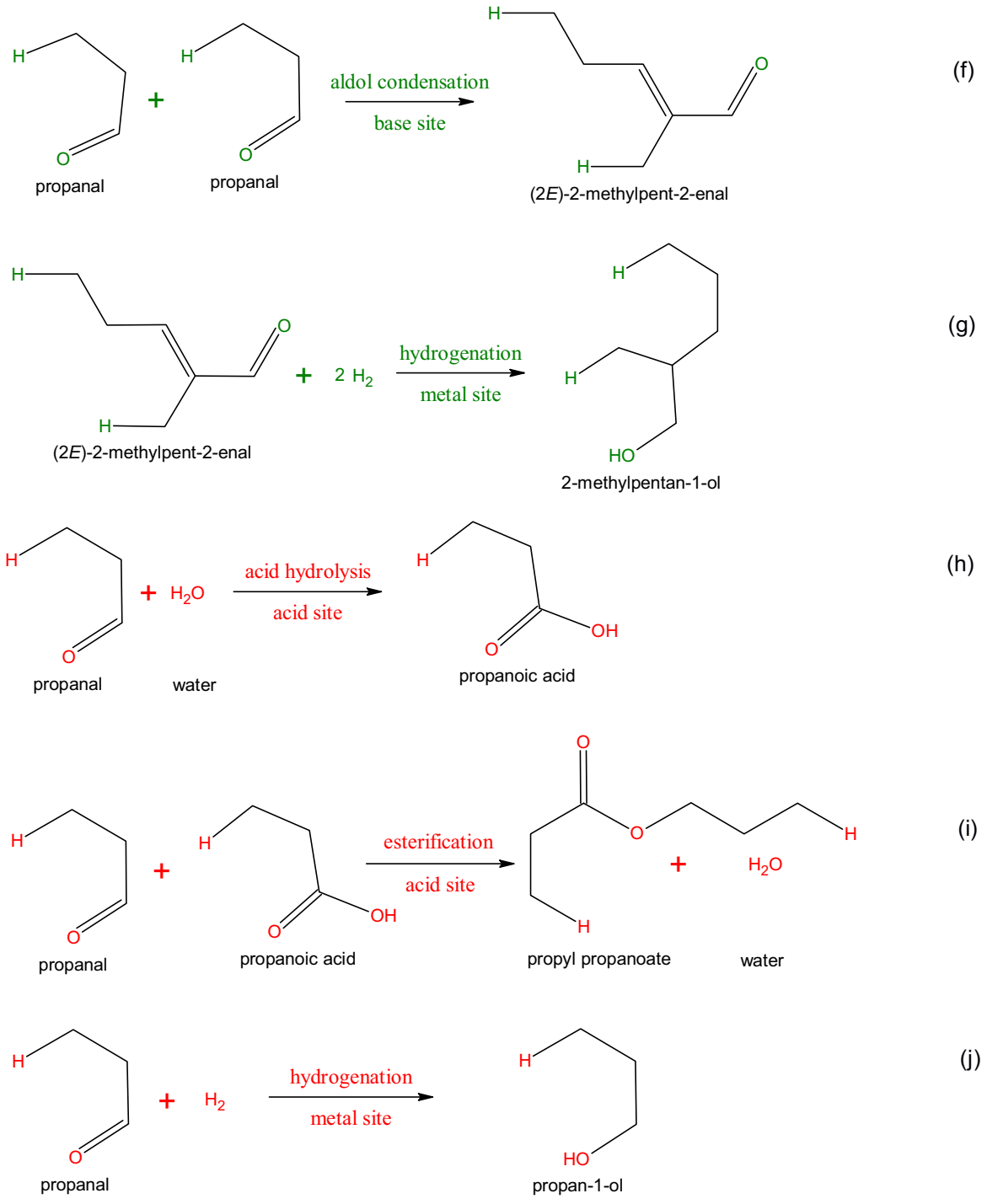

Scheme 3. Consecutive and parallel reactions occurring during one pot synthesis of 2-MP from n-propanol.

propanal and propanoic acid to form propyl propanoate (reaction i) and hydrogenation of *n*-propanal to form propanal (reaction j). The instantaneous selectivity equation was derived for the 2-MP synthesis with similar mathematical derivation as derived for 2-EH synthesis. The equation was derived as:

$$S_{\left(\frac{f}{h+i+j}\right)} = \frac{\dfrac{k_7 K_{Ib}^2 C_I^2 C_{tb}^2}{\left(1+K_{Ib}C_A+K_{Jb}C_J\right)^2}}{\left(\dfrac{k_{10}K_{Ia}K_X C_A C_X + k_{11}K_{Ia}K_M C_I C_M)C_{ta}^2}{(1+K_{Ia}C_I+K_X C_X+K_M C_M+K_N C_N)^2} + \dfrac{k_{12}K_{Im}C_I\sqrt{K_D C_D}C_{tm}^2}{\left(1+K_{Im}C_I+K_{Jm}C_J+K_K C_K+\sqrt{K_D C_D}+K_L C_L+K_O C_O\right)^2}\right)} \quad (26)$$

The parity plot (Fig. ES9) and residual plot for theoretical instantaneous selectivity of 2-MP also validated the derived equation (Fig. ES10). Low selectivity was obtained for 2-MP as compared to 2-EH (Fig. 9). This might be due to easy passage of reactants and products in 2-MP synthesis to the active sites in narrow pores as compared to 2-EH synthesis. The smaller size of molecules accelerated the

Please cite this article in press as: S.C. Patankar, G.D. Yadav, Cascade engineered synthesis of 2-ethyl-1-hexanol from *n*-butanal and 2-methyl-1-pentanol from *n*-propanal using combustion synthesized Cu/Mg/Al mixed metal oxide trifunctional catalyst, Catal. Today (2017), http://dx.doi.org/10.1016/j.cattod.2017.01.008

rate of reaction in 2-MP synthesis (Table ES2). However, due to the higher rate of reaction, the side products were also formed resulting in lower selectivity. Comparison of the values of adsorption constants for 2-EH and 2-MP synthesis at same temperature shows that the adsorption of *n*-propanal was stronger on active sites than adsorption of *n*-butanal on the active sites (Table ES3).

Similar experiments were done for 2-MP as 2-EH synthesis after ensuring that there was no external mass transfer resistance and intra-particle diffusion resistance. Experiments were done by varying the catalyst loading from 0.025 to 0.075 g/cm^3 (Fig. ES8) and by varying the temperature from 110° to 170 °C (Fig. ES9). The activation energy was found to be 10.5 kcal/mol (Table ES2).

4. Conclusion

One pot synthesis of 2-EH was achieved starting from *n*-butanal with 90% selectivity at the beginning of the reaction in solventless conditions. Similar study was conducted on the synthesis of 2-MP starting from *n*-propanal which resulted in 53% selectivity. The pore size of the 5% Cu/MMO catalyst and molecule size played an important role in synthesis. The values of reaction rate constants were calculated for different reactions occurring during one pot 2-EH and 2-MP synthesis. Aldol condensation was found to be the rate controlling step in both the cases with 9.11 and 10.57 kcal/mol, for synthesis of 2-EH and 2-MP, respectively.

Conflict of interest

Authors declare no conflict of interest.

Acknowledgements

S.C. Patankar acknowledges UGC for awarding SRF under its SAP program (Centre of Advanced Studies in Chemical Engineering). G.D. Yadav acknowledges support from the R.T. Mody Distinguished Professor Endowment and J.C. Bose National Fellowship of Department of Science and Technology, Govt. of India. The authors acknowledge the support provided by Dr. Scott Renneckar at University of British Columbia, Vancouver, Canada for the TEM characterization.

Appendix A. Supplementary data

Supplementary data associated with this article can be found, in the online version, at http://dx.doi.org/10.1016/j.cattod.2017.01.008.

References

[1] ICIS. 2-Ethyl hexanol (2-EH) uses and market data. ICB Chemical Profile, 20 July 2009. Available from: URL: www.icis.com/resources/news/2007/11/05/9075782/2-ethylhexanol-2-eh-uses-and-market-data.
[2] S. Gangoli, The Dictionary of Substances and Their Effects, 2nd ed., Royal Society of Chemistry, London, 1999, pp. 523.
[3] Marketsandmarkets.com. 2-Ethyl hexanol (2-EH) by applications (Plasticizers, 2-EH acrylate, 2-EH nitrate, and others) & geography- trends and forecasts to 2018. CH 2364, April 2014. Available from: URL: www.marketsandmarkets.com/Market-Reports/2-ethylhexanol-market-152484808.html.
[4] Chemicals and petrochemicals statistics at a glance: Statistics and Monitoring Division. MLCPCSTAT 14. New Delhi: Department of Chemicals and Petrochemicals (2014).
[5] GlobalData. 2-Ethylhexanol (2-EH) industry outlook in India to 2016 – Market size, company Share, price trends, capacity forecasts of all active and planned plants. 2132350, April 2012. Available from: URL: www.researchandmarkets.com/research/l9rbr4/2ethylhexanol_2.
[6] H. Weissermel, J. Arpe, Industrial Organic Chemistry, Wiley VCH, Weinheim, 2003, pp. 127–144.
[7] R. Tudor, M. Ashley, Platinum Met. Rev. 51 (2007) 164–171.
[8] C.R. Greene, Oxo process using cobalt carbonyl and tertiary phosphine under basic conditions, US Patent, 3278612, 1966 Oct 11, to Shell Oil Company, New York.
[9] A. Chauvel, G. Lefebvre, Petrochemical Processes, Editions Technip, Paris, 1989, pp. 91–94.
[10] S. Matar, M.J. Mirbach, H.A. Tayim, Catalysis in Petrochemical Processes, Kluwer Academic Publishers, Dordrecht, 1989, pp. 128–137.
[11] C.E. Loeffler, L. Stautzenberger, J.D. Unruh, Butyraldehydes and butyl alcohols, in: J.J. Mcketta, W.A. Cunningham (Eds.), Encylopedia of Chemical Processing and Design, vol. 5, New York, Marcel Dekker Inc, 1978, pp. 385–405.
[12] N. Liang, X. Zhang, H. An, X. Zhao, Y. Wang, Green Chem. 17 (2015) 2959.
[13] G.D. Yadav, G.P. Fernandes, Catal. Today 207 (2013) 162–169.
[14] S.M. Doke, G.D. Yadav, Clean Technol. Environ. Policy 18 (1) (2016) 139–149.
[15] G.D. Yadav, B.A. Gawade, Catal. Today 207 (2013) 145–152.
[16] G.D. Yadav, N.P. Ajgaonkar, A. Varma, J. Catal. 292 (2012) 99–110.
[17] S.M. Doke, G.D. Yadav, Chemosphere 117 (2014) 760–765.
[18] A.A. Voskanyan, K.Y. Chan, C.V. Li, Chem. Mater. 28 (8) (2016) 2768–2775.
[19] L.H. Reddy, G.K. Reddy, B. Thirupathi, B.M. Reddy, Curr. Catal. 1 (3) (2012) 164–170.
[20] S.L. Cortes, F.E. Imbert, App. Catal. A: Gen. 452 (2013) 117–131.
[21] Z. Shi, S. Zhang, X. Xiao, D. Mao, G. Liu, Catal. Sci. Technol. 6 (2016) 3457–3467.
[22] L. Chmielarz, P. Kustrowski, A.R. Lasocha, D. Mayda, R. Dziembaj, App. Catal. B: Environ. 35 (2002) 195–210.
[23] X. Huang, C. Atay, T.I. Koranyi, M.D. Boot, E.J.M. Hensen, ACS Catal. 5 (2015) 7359–7370.
[24] Z. Jiang, Z. Hao, J. Yu, H. Hou, C. Hu, J. Su, Catal. Lett. 99 (3–4) (2005) 157–163.
[25] G.D. Yadav, S.C. Patankar, One pot synthesis of oxo-alcohols using heterogeneous catalyst, Indian Patent 4701/MUM/2014, 2014 Dec 19 and PCT/IN2015/000455, 2015 Dec 19.
[26] Y. Shanmugan, L.F. Yuan, C.T. Huei, Y.C. Tih, J. Phys. Chem. B 107 (2003) 1044–1047.
[27] C.C. Addison, N. Logan, Anhydrous Metal Nitrates: Advances in Inorganic Chemistry and Radiochemistry, vol. 6, Academic Press, New York, 1964, pp. 71–142.
[28] F. Marquez, A.E. Palomares, F. Rey, A. Corma, J. Mater. Chem. 11 (2001) 1675–1680.
[29] I.J. Shanon, F. Rey, G. Sankar, J.M. Thomas, T. Maschmeyer, A.M. Waller, A.E. Palomores, A. Corma, A.J. Dent, G.N. Greaves, J. Chem. Soc. Faraday Trans. 92 (21) (1996) 4331–4336.
[30] G. Carja, R. Nakamura, H. Niiyama, App. Catal. A Gen. 236 (2002) 91–102.
[31] S. Kannan, C.S. Swamy, Catal. Today 53 (1999) 725–737.
[32] A. Alejandre, F. Medina, X. Rodriguez, P. salagare, J.E. Sueiras, J. Catal. 188 (1999) 311–324.
[33] K.C. Patil, S.T. Aruna, T. Mimani, Curr. Opin. Solid State Mater. Sci. 6 (2002) 507–512.
[34] A. Varma, A.S. Mukasyan, A.S. Rogachev, K.V. Manukyan, Chem. Rev. Article ASAP (2016), http://dx.doi.org/10.1021/acs.chemrev.6b00279.
[35] M.R. Othman, N.M. Rasid, W.J.N. Fernando, Microporous Mesoporous Mater. 93 (1–3) (2006) 23–28.
[36] T. Baskaran, J. Christopher, A. Sakthivel, RSC Adv. 5 (2015) 98853–98875.
[37] Q. Jiao, H. Liu, Y. Zhao, Z. Zhang, J. Mater. Sci. 44 (2009) 4422–4428.
[38] G.D. Yadav, P.A. Chandan, Catal. Today 237 (2014) 47–53.
[39] M. Mokhtar, S.N. Basahel, Y.O. Al-Angary, J. Alloys Compd. 493 (2010) 376–384.
[40] M. Zhou, Z. Zeng, H. Zhu, G. Xiao, R. Xiao, J. Energy Chem. 23 (1) (2014) 91–96.
[41] K. Yan, J. Liao, X. Wu, X. Xie, RSC Adv. 3 (2013) 3853–3856.
[42] J. Barrault, A. Derouault, G. Courtois, J.M. Maissant, J.C. Dupin, C. Guimon, H. Martinez, E. Dumitriu, App. Catal. A Gen. 262 (1) (2004) 43–51.
[43] M.M. Villaverde, T.F. Garetto, A.J. Marchi, Catal. Comm. 58 (2015) 6–10.

Please cite this article in press as: S.C. Patankar, G.D. Yadav, Cascade engineered synthesis of 2-ethyl-1-hexanol from *n*-butanal and 2-methyl-1-pentanol from *n*-propanal using combustion synthesized Cu/Mg/Al mixed metal oxide trifunctional catalyst, Catal. Today (2017), http://dx.doi.org/10.1016/j.cattod.2017.01.008